U-Pb zircon geochronology of a tholeiitic intrusion and associated migmatits at a continental crust-mantle transition, Val Malenco, Italy

Autor(en): **Hansmann, Werner / Müntener, Othmar / Hermann, Jörg**

Objekttyp: **Article**

Zeitschrift: **Schweizerische mineralogische und petrographische Mitteilungen = Bulletin suisse de minéralogie et pétrographie**

Band (Jahr): **81 (2001)**

Heft 2

PDF erstellt am: **24.09.2024**

Persistenter Link: https://doi.org/10.5169/seals-61691

SCHWEIZ. MINERAL. PETROGR. MITT. 81, 239–255, 2001

Dedicated to Volkmar Trommsdorff on the occasion of his 65th birthday

U–Pb zircon geochronology of a tholeiitic intrusion and associated migmatites at a continental crust-mantle transition, Val Malenco, Italy

by *Werner Hansmann*[1], *Othmar Müntener*[2,3] and *Jörg Hermann*[2,4]

Abstract

This paper provides new constraints on the crystallisation age of the gabbroic rocks and associated migmatites that are exposed now along the boundary of the Penninic and Austroalpine nappes in the Eastern Central Alps (Val Malenco, N Italy). The gabbros intruded at the crust-to-mantle boundary and caused granulite facies metamorphism in the country rocks. Zircons were extracted from the gabbros and metagabbros as well as from an associated leucogranite and single crystals were dated by the U–Pb method. In addition the lead isotopic composition was determined on plagioclase separated from the same samples.

One Fe-gabbro with preserved primary mineral assemblage yielded sufficient zircons suited for U/Pb dating. Additionally a Zr-rich Ti-Fe-gabbro which is overprinted by Alpine metamorphism and a leucogranite representing local anatexis of country rocks during the gabbro intrusion were selected for dating. 15 U–Pb data points of the U-poor (30–150 ppm) zircons from both gabbros yielded an upper concordia intersection age of 281 ± 19 Ma, whereas 10 U-rich (600–4000 ppm) zircons from the leucogranite define a very similar upper concordia intersection at 278 –2.5/+2.6 Ma corresponding to an Early Permian age. On a regional scale, the Early Permian age of the gabbros is consistent with a major phase of continental crustal growth during the late Paleozoic.

Plagioclase of all but one sample of the tholeiitic gabbro suite is characterised by a Pb isotopic composition typical for average crust. The relatively homogeneous Pb isotopic composition of these rocks, which is independent of the degree of differentiation, suggests a contaminated mantle source of their parental magma rather than crustal contamination during the emplacement at the crust-to-mantle boundary.

One Ti-Fe-gabbro dike showed elevated μ and ω values ($\mu = 9.98$; $\omega = 40.3$) very similar to those of the anatectic leucogranite. Contamination of this rock most likely took place during its intrusion into metasedimentary country rocks. U/Pb results of some zircons of an other Ti-Fe-gabbro suggest the presence of inherited crustal components. Abundant zircon and a high Zr content (603 ppm) indicate that the magma of this sample was saturated with zircon and thus xenocrystic zircon may have survived. However, the presence of cores or xenocrysts has not been confirmed by optical means yet. Observed cores and the presence of inherited lead in zircons of the leucogranite are in agreement with an anatectic origin of this rock.

Keywords: Geochronology, U–Pb method, zircons, crust-mantle transition, common lead, tholeiitic gabbro, Val Malenco, Eastern Central Alps.

1. Introduction

The association of ultramafic and gabbroic rocks occurring at various locations in the Alps points to initial tectonic settings that are fundamentally different. In one setting gabbros formed part of an ophiolitic complex and represent oceanic crust, for example in the Platta nappe (DIETRICH, 1969; DESMURS et al., 2001) and in the Zermatt–Saas Fee zone (BEARTH, 1967; RUBATTO et al., 1998). In a second setting, gabbros intruded mantle rocks during rifting and were integrated in the conti-

[1] Institut für Isotopengeologie und Mineralische Rohstoffe, ETH Zentrum, CH-8092 Zürich, Switzerland. <werner.hansmann@erdw.ethz.ch>

[2] Institut für Mineralogie und Petrographie, ETH Zürich, ETH Zentrum, CH-8092 Zürich, Switzerland.

[3] Present address: Geological Institute, University of Neuchâtel, Rue Emile-Argand 11, CH-2007 Neuchâtel, Switzerland.

[4] Present address: Research School of Earth Sciences, ANU, Canberra 0200, Australia.

nent-ocean transition of passive continental margins (LEMOINE et al., 1987). Contrastingly, gabbroic intrusions associated with ultramafic and granulitic rocks at deep levels of the continental crust (e.g. Ivrea zone) have been interpreted to result from magmatic underplating (e.g. VOSHAGE et al., 1990).

The serpentinite mass of Val Malenco (East Central Alps) forming the largest ultramafic body in the Penninic domain, has been considered to be part of a Mesozoic ophiolite since STAUB's (1922) report. Subsequent observations, such as the presence of ophicarbonates (GYR, 1967; TROMMSDORFF and EVANS, 1977), overlying pillow basalts (MONTRASIO, 1973) covered by an oceanic sedimentary sequence with Mn mineralisations (FERRARIO and MONTRASIO, 1976; PERETTI, 1985), have lent further support to this hypothesis. However, an initial ophiolitic setting of an associated gabbroic complex ("Fedoz gabbro") was rejected by GAUTSCHI (1979, 1980) on the basis of field relations and its high-pressure metamorphic evolution documented in coronas between plagioclase and olivine. Detailed field studies (SPILLMANN 1989,1993; TROMMSDORFF et al., 1993; MÜNTENER and HERMANN, 1996; HERMANN and MÜNTENER, 1996; ULRICH and BORSIEN, 1996) then revealed that the relations between this gabbroic complex and the ultramafics as well as its metasedimentary country rocks were of crucial importance to the understanding of the origin and evolution of the Malenco serpentinites. Primary igneous contacts between the gabbros and the metasedimentary basement (SPILLMANN 1989, 1993; TROMMSDORFF et al., 1993; MÜNTENER and HERMANN, 1996; ULRICH and BORSIEN, 1996) as well as between the gabbros and the ultramafic rocks (TROMMSDORFF et al., 1993; HERMANN et al., 1993; MÜNTENER and HERMANN, 1996; ULRICH and BORSIEN, 1996) plus partially preserved pre-Alpine metamorphic mineral assemblages of granulite facies grade in these rock units led to the conclusion that the gabbros intruded at the crust-to mantle boundary and that the Malenco serpentinites originally represented a fragment of the subcontinental upper mantle (TROMMSDORFF et al., 1993; HERMANN et al., 1997). The "ophiolitic" appearance of the Malenco ultramafic rocks then resulted from later exhumation and denudation in an oceanic environment at the Adriatic continental margin during Jurassic rifting (TROMMSDORFF et al., 1993).

For the understanding of the pre-Alpine evolution of the Adriatic crust and underlying lithospheric mantle the intrusion age of the gabbroic complex is of great importance in several respects (i) The gabbro intrusion reflects partial melting of rising asthenosphere in connection with extension of the overlying lithosphere (TROMMSDORFF et al., 1993) and thus indicates a period of extensional tectonics (e.g. DAL PIAZ, 1993). (ii) The emplacement of the gabbroic complex welded upper mantle and lower crustal rocks and thus marked the younger age boundary for the common evolution of this crust-to-mantle section. (iii) Field relations also suggest that the gabbro intrusion caused granulite grade metamorphism and partial melting of the lower crustal rocks in its vicinity (TROMMSDORFF et al., 1993; MÜNTENER and HERMANN, 1996).

Based on field relationships alone the upper age limit for the gabbroic intrusion has been estimated to be late Variscan (SPILLMANN, 1989; SPILLMANN and BÜCHI, 1993) to post-Variscan (TROMMSDORFF et al., 1993) whereas the lower age boundary was estimated to be Mesozoic (SPILLMANN and BÜCHI, 1993). Geochronologic data on the Malenco area document mostly Alpine events (JÄGER and HUNZIKER, 1969; HUNZIKER et al., 1992; DEUTSCH, 1983; HANDY et al., 1996; VILLA et al., 2000) or the later cooling history (JÄGER and HUNZIKER, 1969; WAGNER et al., 1977). In order to gain insight into the earlier evolution of the Malenco rocks this study focuses on promising samples from the Monte Braccia–Lago Pirola area, where pre-Alpine mineral assemblages are still preserved and the geochronometers may not have been affected too strongly by the Alpine history.

Age determinations on several pre-Alpine gabbroic intrusions in the Alpine realm yielded data between ca. 300 and 270 Ma that fall within the age interval estimated for the Malenco gabbro complex. Such intrusions are represented by the following gabbros: Ivrea zone of 285 Ma (U/Pb on zircons; PIN, 1986), Matterhorn and Mont Collon of 284 ± 0.7 Ma (MONJOIE et al., 2001), Monte Mucrone of 285 ± 7 Ma (RUBATTO et al., 1999), and Sondalo gabbroic complex of 270 Ma (U/Pb on zircons; BACHMANN and GRAUERT, 1981) and 280–300 Ma respectively (Sm/Nd mineral isochron ages; TRIBUZIO et al., 1999). The post-Variscan intrusion of these gabbros has been interpreted to result of the change from compressional tectonics during the Variscan orogeny towards an extensional regime (DAL PIAZ, 1993).

In this paper we present zircon U/Pb results obtained on two members of the gabbroic suite from Val Malenco. Problems arising from conventional U–Pb zircon dating of tholeiitic gabbros are discussed and a way to circumvent them has been tested by U/Pb dating of zircons from an associated leucogranite derived by local anatexis caused by the gabbroic intrusion. Pb isotope data of plagioclase are also given for the dated samples

and additional ones. These have been used for the common lead correction of zircon data and showed to be helpful in the discussion about zircon inheritance. They further allowed a Pb isotopic characterisation of the studied samples and a comparison with other Alpine tholeiites.

2. Geologic Setting

The study area is located in Val Malenco (N Italy), at the border zone to SE Switzerland (Fig. 1). In the Val Malenco the Penninic-Austroalpine boundary is composed of three main units, (a) the Penninic Malenco ultramafics, (b) the Forno "ophiolitic" suite, and (c) the Austroalpine Margna nappe.

The Malenco unit is dominated by a large serpentinized ultramafic body which is mainly composed of various (partially preserved) peridotitic and subordinate pyroxenitic rocks (MÜNTENER and HERMANN, 1996). The ultramafic rocks underlie granulite grade metasedimentary rocks present as kyanite-garnet gneisses showing local melt segregation (MÜNTENER and HERMANN, 1996; HERMANN, 1997), minor marbles and calcsilicates. Primary contacts between the ultramafics and the above crustal granulites have not been reported. However, these two units were welded by a gabbro intrusion, fixing this transition from mantle to lower crustal rocks. The gabbros show primary contacts (crosscutting dikes and engulfed xenoliths in the gabbro) with the Malenco ultramafics and the overlaying granulites at several locations (TROMMSDORFF et al., 1993; MÜNTENER and HERMANN, 1996). Partial melting in the granulites produced leucogranites which locally intruded gabbroic dikes crosscutting the lower crus-

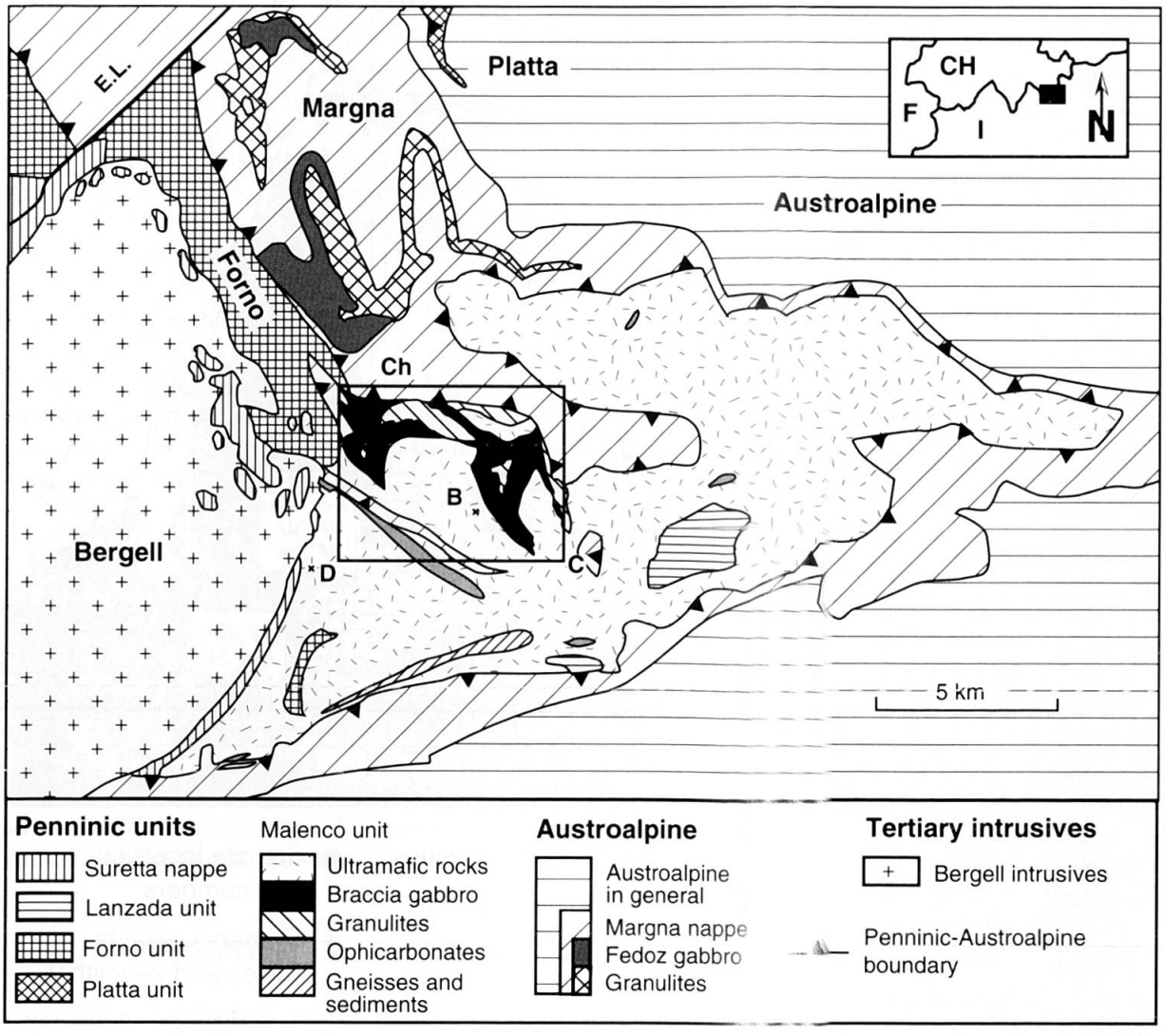

Fig. 1 Tectonic map of the Penninic-Austroalpine boundary in Val Malenco (N Italy), modified from MÜNTENER and HERMANN (1996). The inset in the upper right corner shows the geographic position of this area at the Swiss-Italian border zone. The frame outlines the study area which is shown in more detail in figure 2. B = Monte Braccia, D = Monte Disgrazia, C = Chiesa, Ch = Chiareggio, E.L. = Engadine Line

tal rocks (MÜNTENER and HERMANN, 1996; HERMANN et al., 1997). These field relations suggest that gabbro intrusion and partial melting of the lower crust were closely related. The magmatic evolution of the tholeiitic gabbro suite passed from Mg-gabbros via Fe-gabbros to quartz-diorites and to highly differentiated Fe-Ti-P-rich diorites (HERMANN et al., 2001). In the western part of the Malenco ultramafics ophicarbonate rocks (TROMMSDORFF and EVANS, 1977) occur. The presence of rodingitized mafic dikes and the stable isotope signature of the ophicarbonates (BURKHARD and O'NEILL, 1988; POZZORINI and FRÜH-GREEN, 1996) indicate that metasomatism and metamorphism took place in an oceanic environment.

In their western part the Malenco ultramafics are crosscut by MOR type basaltic dikes of the Forno unit (Fig. 1). This unit is composed of metamorphosed elements of a sea floor sequence (PUSCHNIG, 2000): locally preserved pillow basalts and pillow breccias (MONTRASIO, 1973) overlain by sediments of presumably Jurassic age (PER-

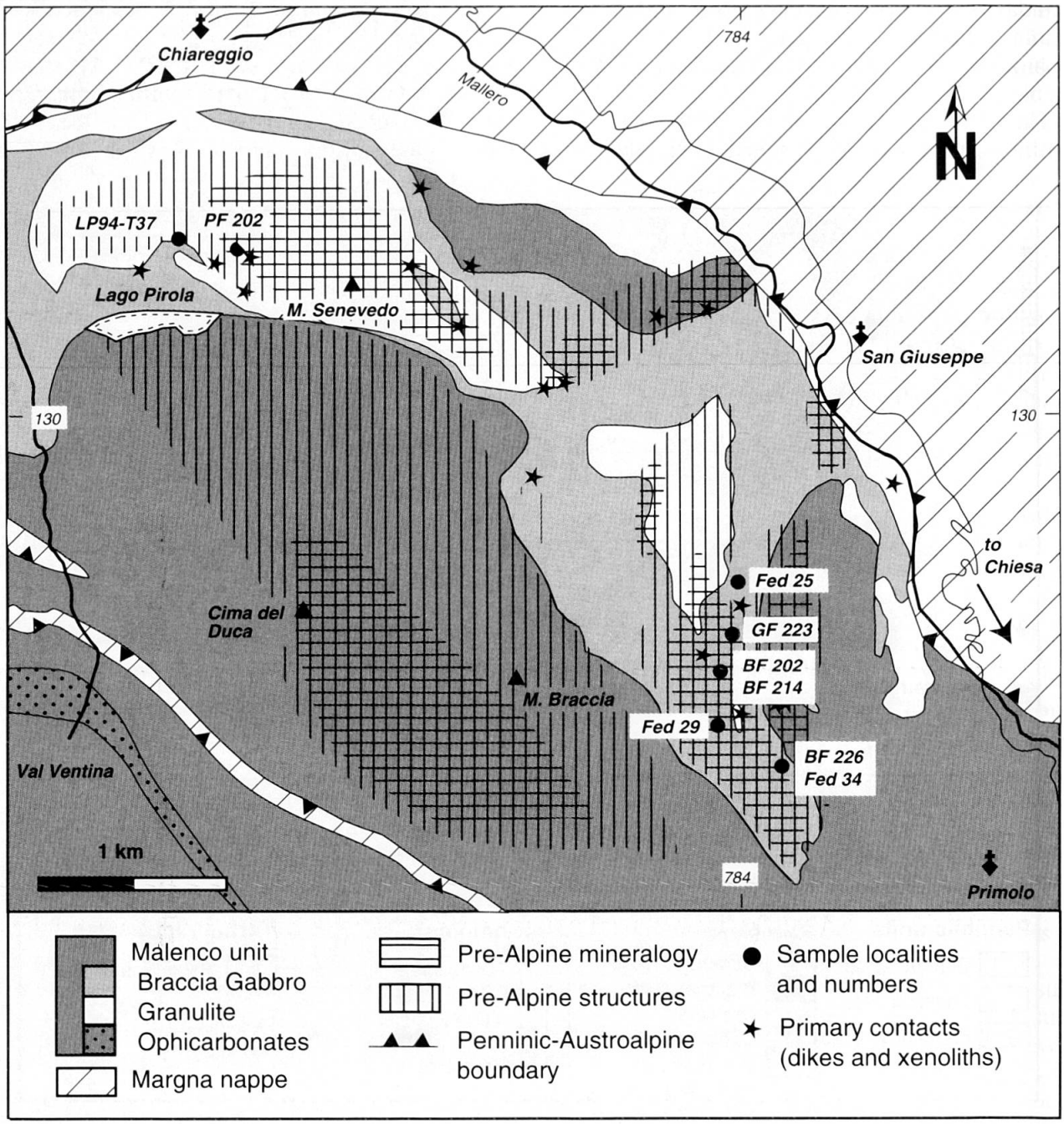

Fig. 2 Simplified geologic map of the Monte Braccia–Lago Pirola area, where pre-Alpine structures and mineral assemblages are preserved (modified from MÜNTENER and HERMANN, 1996). Their major occurrences are marked in the map by signatures. Samples locations are shown by dots.

ETTI, 1985) containing quartzites (probably metaradiolarites) with manganese mineralisations (FERRARIO and MONTRASIO, 1976).

The lower Austroalpine Margna nappe is composed of lower crustal rocks which are mainly represented by a banded metasedimentary sequence (Fedozserie of STAUB, 1946) and metagabbros (Fedozer Gabbro) as well as upper crustal rocks (granitoid orthogneisses and metasediments) and their sedimentary cover. A tectonic contact separates the lower and upper crustal units of the Margna nappe (SPILLMANN, 1993). Relics of high-grade pre-Alpine mineral parageneses still are preserved within the metasediments of the lower crustal unit of the Margna nappe (GUNTLI and LINIGER, 1989; SPILLMANN, 1993).

A paleogeographic reconstruction shows that during the Jurassic the Margna and Malenco/Forno units formed a continent-ocean transition from the Adria continental margin towards the Piemont-Ligurian basin. In this setting a part of Malenco ultramafics represented a fragment of subcontinental mantle which formerly underlaid the Adriatic crust (TROMMSDORFF et al., 1993) and became denudated during Jurassic rifting. The peridotitic subcontinental rocks as well as the attached gabbros and lower crustal metasediments show the same retrograde metamorphic path from the high grade conditions at the crust-mantle boundary to the suboceanic environment (MÜNTENER et al., 2000).

During the Alpine convergence the Austroalpine units were stacked into a nappe pile, which then was thrust over the Penninic units. In the Malenco area the Alpine metamorphism reached epidote-amphibolite conditions (0.5–0.7 GPa and 450–500 °C; GUNTLI and LINIGER, 1989; HERMANN, 1997). Despite this medium grade Alpine metamorphism several lenses of Malenco ultramafics and attached lower crustal rocks preserved pre-Alpine high-grade mineral assemblages. These lenses are located in the Monte Braccia–Lago Pirola area (Fig. 2). Gabbroic rocks from this area have recently been termed "Braccia gabbro" (e.g. HERMANN, 1997). The preferred use of this term rather than "Fedozer Gabbro" is explained in MÜNTENER and HERMANN (1996, p. 481) and HERMANN and MÜNTENER (1996, p. 506).

3. Analytical notes

Zircons were separated using standard techniques: Wilfley table, magnetic separator, methylene jodide, Clerici's solution. Zircon yields varied strongly. Hand specimens (300–400 g) of leucogranite LP94-T37 and Ti-Fe-gabbro BF202 each yielded > 100 mg of zircon, whereas only 14 mg could be extracted out of 52 kg of gabbro Fed29. Small splits of the zircon populations were embedded in piperine for microscopic examination and groups of representative crystals were selected for cathodoluminescence (CL) imaging. They were mounted in epoxy resin and polished. A part of the zircons to be dated were air-abraded using the technique described by KROGH (1982).

Selected single zircons and two small grain fractions were ultrasonically cleaned in acetone. After rinsing with distilled water they were further treated with warm (80 °C) 3N nitric acid for 60 min. Analyses of some of these wash solutions showed that mainly common Pb was removed and that the portions of radiogenic Pb and U leached from the samples were < 0.3%, except for the U-rich sample LP94-10. For this sample the analytical data of the sample and the leach solution were combined. Zircon dissolution and extraction of U and Pb was done applying minimised versions of the methods of KROGH (1973). For feldspar dissolution and Pb separation the procedures given by KÖPPEL et al. (1997) were applied. Mass spectrometric analyses with the Varian MAT tandem instrument followed the procedures described by OBERLI et al. (1981) and BOSSART et al. (1986). The following fractionation factors ($F = 1 + \Delta_{a.m.u.} \times f$) were applied for the data reduction: $f = 0.07 \pm 0.05$ per atomic mass unit (a.m.u.) for Pb and 1.0 ± 1.0 per a.m.u. for U. From two zircons U and Pb, as well as Pb from the feldspars were analysed with the Finnigan MAT 262 mass spectrometer equipped with an ion counting system. For this instrument f was determined to be $0.13 \pm 0.04\%$ per a.m.u. for Pb and $0.1 \pm 0.04\%$ per a.m.u. for U. Data reduction and error treatment were performed following the algorithm given by RODDICK (1987). Pb blanks decreased during the interval of analytical work from 15 to 10 ppm; the U blank was considered as negligible. The Pb composition of the blank was $^{206}Pb/^{204}Pb = 18.22 \pm 3.6\%$; $^{207}Pb/^{204}Pb = 15.56 \pm 2.0\%$ and $^{208}Pb/^{204}Pb = 37.87 \pm 2.8\%$. Common lead associated with the zircons (inclusions, intergrowths) was corrected using the composition determined on plagioclase from the host rocks of the zircons and in one case (BF202) the common lead composition was calculated using the model of STACEY and KRAMERS (1975). All errors given with analytical data, in tables and on the diagrams are at the 2 σ level.

4. Samples

In the Monte Braccia–Lago Pirola area four different primary rock types have been distin-

guished within the gabbroic complex (MÜNTENER and HERMANN, 1996): (1) a coarse-grained gabbro-norite (Mg-gabbro) with flaser texture is the dominant lithology. (2) Less frequent is a coarse-medium grained amphibole ilmenite gabbro-norite (Fe-gabbro). (3) Medium grained ilmenite pyroxene amphibole gabbros (Ti-Fe-gabbro) occur mainly as rare dikes. (4) Rare dikes of quartz diorite crosscut the Fe-gabbros. The detailed field relations of these rocks are given by MÜNTENER and HERMANN (1996) and HERMANN (1997).

The magmatic differentiation and geochemical characteristics of this tholeiitic rock suite are discussed by HERMANN et al. (2001). Major and

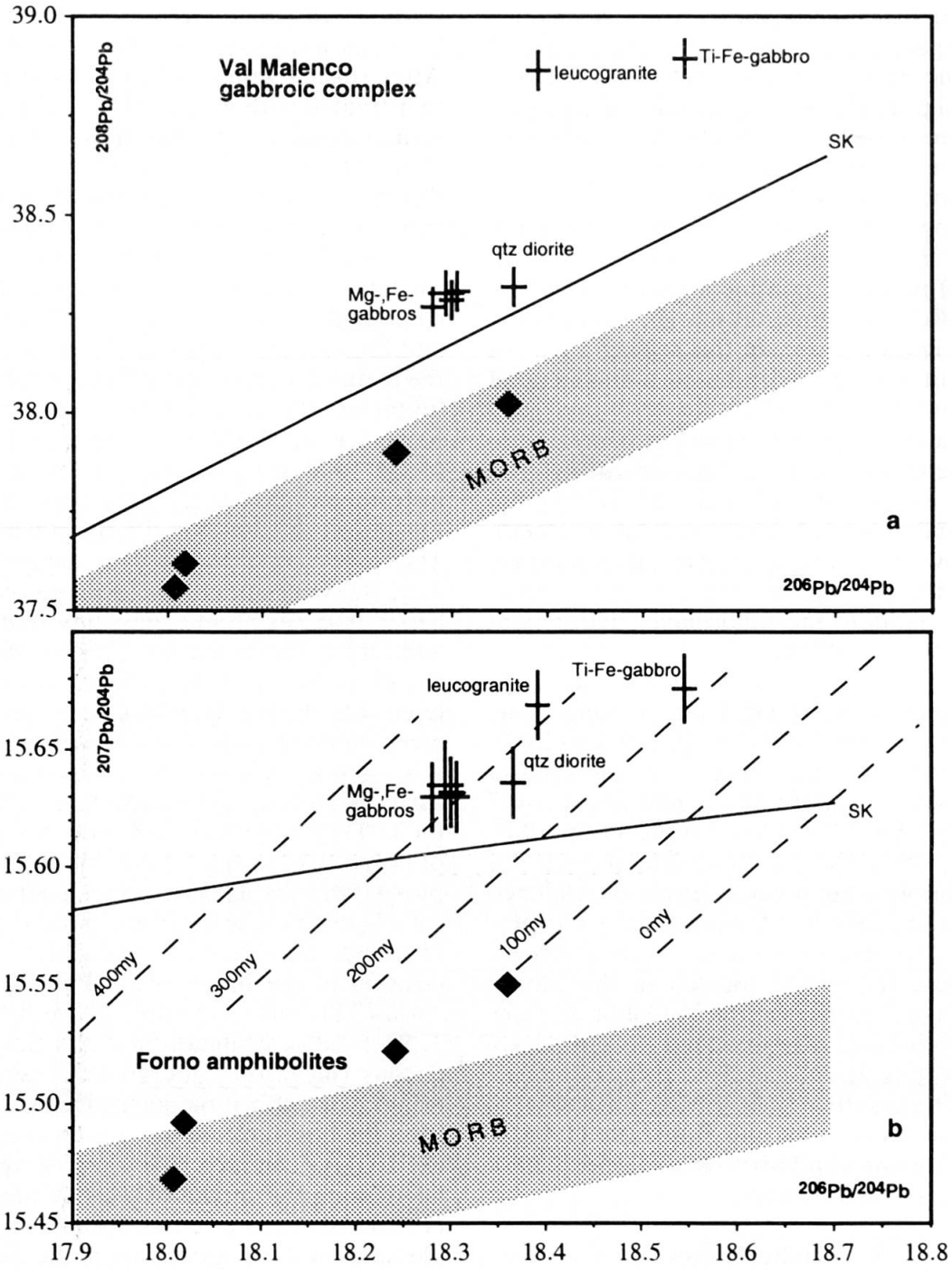

Fig. 3 Pb isotope data of feldspar from Val Malenco gabbroic rocks and the anatectic leucogranite. (a) $^{208}Pb/^{204}Pb$ versus $^{206}Pb/^{204}Pb$ and (b) $^{207}Pb/^{204}Pb$ versus $^{206}Pb/^{204}Pb$ diagrams. The field for MORB, mineral data from the adjacent Forno amphibolites (represented by diamonds, PERETTI and KÖPPEL, 1986) and the evolution curves (labelled SK) for average crustal lead (μ = 9.74, ω = 36.84; STACEY and KRAMERS, 1975) are given for comparison. The Pb isochrons shown in (b) are calculated on the basis of the Pb evolution model of STACEY and KRAMERS (1975). Note, that the Ti-Fe-gabbro represents a dike crosscutting metasedimentary rocks.

trace element data of the analysed samples are listed in HERMANN (1997). Here the Pb isotopic data of the samples are added and briefly discussed, since the lead isotope compositions of their feldspars were used for the correction of the zircon U/Pb data.

4.1. PETROGRAPHIC DESCRIPTION

Fed29 (Fe-gabbro): In situ sample (Swiss coordinates: 783'870/128'330). It consists of the primary phases plagioclase, clinopyroxene, orthopyroxene, Ti-pargasite, ilmenite, green spinel and apatite. Plagioclase (An_{50}; HERMANN, 1997) is variably dusty and some pyroxenes are rimmed by alteration products. Along rare fine actinolite–chlorite–quartz–calcite veins plagioclase and pyroxenes are strongly altered. Despite a bulk 145 ppm Zr content in this rock, no zircons are detected in thin section. This may largely be explained by Zr control due to precipitating pyroxenes (cf. POLDERVAART, 1956). In clinopyroxenes of Fe-gabbro samples Zr contents of up to 345 ppm were determined (HERMANN et al., 2001).

BF202 (Ti-Fe-gabbro): From a 15 cm thick dike within Fe-gabbros (783'890/128'620). This rock shows a distinct foliation, which is interpreted to reflect the Alpine deformation during which the dike reacted as a deformation horizon within the more rigid undeformed Fe-gabbros. Although the primary phases (except apatite) have been replaced by an Alpine metamorphic mineral assemblage of garnet, actinolitic amphibole, chlorite, rutile, ilmenite and quartz this sample was chosen for dating because of its considerable zircon contents (ca. 30 crystals in a 10 cm^2 thin section). The unusually high bulk Zr concentration of 603 ppm probably reflects the high degree of differentiation of this rock type (HERMANN et al., 2001) and may explain that zircon saturation was attained during magmatic crystallisation of this sample. No plagioclase was found in this rock.

PF202 (Ti-Fe-gabbro). From a 0.5–1.0 m thick dike crosscutting granulitic metapelites (781'380/130'870). It is the same dike as PF203 of HERMANN et al. (2001). Primary plagioclase is preserved to a large degree, whereas pyroxenes are amphibolised and brown Ti pargasite partially shows fine rims of green amphibole. Ilmenite and apatite occur frequently.

LP94-T37 (leucogranite) This sample was collected from a leucogranite within the Mg-gabbro close to the contact between gabbro and metapelites (781'020/130'940). The leucogranite represents local partial melts derived from the metapelitic country rocks of the gabbro (MÜNTENER and HERMANN, 1996; ULRICH and BORSIEN, 1996). LP94-T37 is composed mainly of large grains of recrystallised quartz, albitic plagioclase and K-feldspar. Plagioclase is partially altered to white mica and clinozoisite. Minor amounts of biotite and muscovite also are present, and recrystallised titanite, pseudomorphs of clinozoisite after garnet, and zircon (120 grains in a thin section) occur as accessories.

Other samples: A pilot mineral separation on a Mg-gabbro proved to be unsuccessful and attempts to separate zircons from a quartz-diorite (Fed34/BF226) and an other Fe-gabbro (Fed25) yielded only few small grains which were not suited for an age determination at the given analytical limitations. Plagioclase was separated for Pb isotope analyses from these samples and two additional Mg-gabbros with preserved pre-Alpine mineralogy.

4.2. PB ISOTOPIC CHARACTERISATION

Lead isotope and concentration data of 6 plagioclase samples from the gabbroic suite and one from an unseparated mixture of albitic plagioclase and alkali feldspar of the leucogranite are listed in table 1. The Pb isotope ratios are not corrected for potential contributions of radiogenic

Tab. 1 Pb isotope composition of plagioclase.

Sample	Rock type	$^{206}Pb/^{204}Pb$	$^{207}Pb/^{204}Pb$	$^{208}Pb/^{204}Pb$	Pb[ppm]
BF214	Mg-gabbro	18.294 (17)	15.635 (18)	38.303 (54)	0.90
GF223	Mg-gabbro	18.306 (12)	15.630 (14)	38.308 (47)	0.63
Fed25	Fe-gabbro	18.300 (11)	15.632 (14)	38.286 (46)	0.88
Fed29	Fe-gabbro	18.280 (11)	15.630 (14)	38.269 (46)	4.18
BF202	Ti-Fe-gabbro	18.545 (11)	15.676 (14)	38.894 (47)	21.4
BF226	Qtz-diorite	18.365 (12)	15.636 (14)	38.319 (47)	1.84
LP94-T37*	Leucogranite	18.391 (11)	15.669 (15)	38.864 (47)	2.96

* Mixture of albitic plagioclase and alkali feldspar.

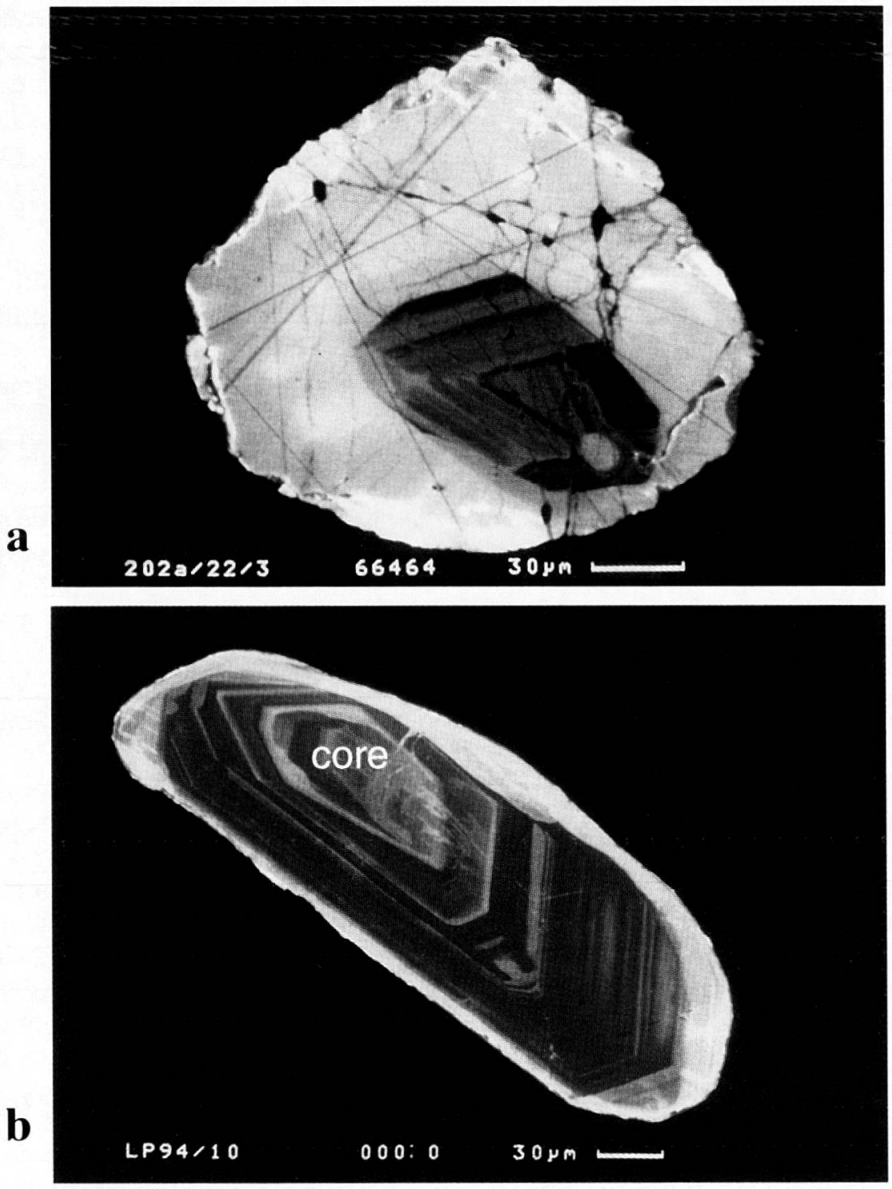

Fig. 4 Cathodoluminescence images of two zircons typical of the very different populations of gabbro BF202 and leucogranite LP94-T37. (a) BF202: A central zircon part showing oscillatory and sector zoning is cut and replaced by large marginal domains characterised by bright CL intensity. (b) LP94-T37: A prismatic crystal with a large oscillatory zoned central part contains a rare corroded core and displays a small rim only of bright CL intensity. Zircons of the gabbro Fed29 show CL images similar to BF202 with a smaller fraction of high CL marginal domains than BF202. In all three zircon populations the oscillatory zoned centres are interpreted as primary magmatic zircon, whereas the high CL outer domains reflect recrystallisation due to Alpine metamorphism.

lead from minor amounts of U and Th present in the plagioclase. However, LA-ICP-MS data (HERMANN et al., 2001) of plagioclase from this rock suite show U/Pb and Th/Pb ratios of <0.0123. Calculation for the largest U/Pb ratio showed that such a correction would amount to a maximum of 0.033 for the most sensitive $^{206}Pb/^{204}Pb$ ratio and thus does not change the overall data pattern obtained for the studied plagioclase.

On the lead/lead isotope ratio diagrams (Figs 3a,b) the four samples from Mg- and Fe-gabbros form a cluster of overlapping data points. Quartz-diorite shows a slightly more radiogenic composition. These data are derived from samples located within the gabbro body. Their μ and ω values ($\mu = {}^{238}U/^{204}Pb$, $\omega = {}^{232}Th/^{204}Pb$) are typical of average crust rather than of a mantle source. The crust-derived leucogranite is characterised by distinctly higher μ and ω values. On a two-stage lead evolution diagram (STACEY and KRAMERS, 1975) the Fe- and Mg-gabbros as well as the leucogranite plot close to a 300 Ma isochron (Fig. 3b) indicat-

ing a Late Paleozoic Pb model age for these rocks which is similar to their Permian age of intrusion (see section 7.2).

In contrast to the other gabbros, the Ti-Fe-gabbro PF202 represents a dike crosscutting the metasedimentary country rocks of the gabbros. This sample has a more radiogenic Pb isotopic composition and is also characterised by higher μ and ω values very similar to those of the leucogranite. The clearly more crustal Pb isotopic signature of the Ti-Fe-gabbro, compared with the other gabbros, most likely resulted from crustal contamination. Its distinct crustal Pb isotope signature combined with the 5 to 30-fold lead concentration of the other gabbroic plagioclase suggests a strong contamination with respect to this element. Since in this dike lead largely is contained in the major magmatic phases plagioclase and Ti pargasite (see data of HERMANN et al., 2001) this contamination must have taken place before or during its intrusion into the metasedimentary rocks. Whether the more radiogenic nature of PF202 plagioclase is also due to the same contamination or reflects contributions of radiogenic lead from apatite inclusions remains unclear.

5. Zircon

Cathodoluminescence (CL) images displaying the most characteristic features of zircon are shown in figures 4a and 4b.

Fed 29: Zircons are generally light-coloured, relatively clear, mainly short prismatic and rounded. Only few crystals show euhedral zircon forms. Some prismatic grains are elongated in directions differing from the c-axis and some are embayed reflecting impeded growth. A part of the grains are broken or display other effects of deformation, like undulatory extinction and internal cracking. Closer inspection reveals several generations of cracks: besides recent cracks due to mineral separation old crack faces are indicated by arrays of numerous secondary fluid inclusions.

BF202: Most of the crystals are equant to short prismatic with rounded edges or even anhedral (Fig. 4a). Crystal surfaces are often uneven or rugged. Some grains show the same features of deformation as zircons of Fed29. Most zircons, however, are mainly turbid due to many internal cracks filled with bubbles and irregularly shaped fluid inclusions. Cracking most likely was caused by the Alpine deformation. Major primary inclusions are apatite and opaque phases.

LP94-T37: Zircons are mainly prismatic (Fig. 4b) and subhedral with rounded edges. Some grains are embayed or show a conspicuous isthmus-like shape. Intergrowths parallel to the c-axis are common. Cracks are filled with fine bubbles. Broken zircons are observed in thin section, though they are less frequent in the grain mount than in the other two samples. Irregularly shaped larger inclusions in the crystals might reflect trapped melt. Cores could not unequivocally be detected in the piperine mount by optical means. Only in one out of 10 grains of the polished epoxy mount a core could be identified by cathodoluminescence imaging (Fig. 4b).

6. U–Pb results

Sample characteristics and U–Pb results of the 3 dated rocks are given in tables 2 and 3. The zircon data of the two gabbroic rocks are shown in figure 5 and the data from the zircons from the anatectic leucogranite are plotted in figure 6.

Due to low U and radiogenic Pb concentrations (e.g. BF202-15, -16, -18) relatively large errors resulted for most of the gabbroic single zircon samples. In addition, some of the zircons contained significant amounts of common lead reaching concentrations as high as radiogenic lead (BF202-5). The common lead correction for such zircons may be problematic if its isotopic composition is not well constrained (e.g. due to several generations of inclusions and intergrowths). In the simple case of non-metamorphic magmatic zircon common lead is associated with inclusions and superficial intergrowths. The Pb composition of cogenetic feldspar usually is considered a good approximation of the common lead in such zircons. In the present study this approximation seems to be justified for gabbro Fed29 and leucogranite LP94-T37, both of which show only minor effects of Alpine metamorphism. The situation of sample BF202, in which there is evidence of Alpine recrystallisation is more complicated: zircons and their primary inclusions represent the first generation, fluid inclusions that formed during the healing of cracks represent an Alpine event as do metamorphic mineral phases intergrown with zircon at its rugged surface.

In order to estimate effects of different common lead compositions on the final results the U/Pb data of the zircons from BF202 were calculated with the common lead composition of Fed29 representing primary gabbroic lead and, alternatively, with an Alpine (100 Ma) composition using the model of STACEY and KRAMERS (1975). Among the abraded samples the $^{207}Pb/^{206}Pb$ ratios of the strongly deviating sample BF202-15 differ by 0.56%, whereas the effects for the other samples are < 0.15%. In the unabraded common lead

enriched samples BF202-5 and BF202-7 the $^{207}Pb/^{206}Pb$ ratios differ by 0.89% and 0.17% respectively, and for the other unabraded samples by < 0.1%. In the less sensitive samples with measured $^{206}Pb/^{204}Pb > 300$ the $^{207}Pb/^{206}Pb$ ratios differ by less than 0.05%. Note, however, that common lead in these zircons probably reflects mixtures of primary (e.g. Fed29) and Alpine common lead, and the actual deviations would be smaller than the above calculated maximum effects. In order to minimise the uncertainties arising from potentially problematic common lead corrections regression ages were also calculated for the relatively insensitive samples with $^{206}Pb/^{204}Pb > 300$ only.

On the $^{207}Pb/^{206}Pb$ versus $^{238}U/^{206}Pb$ (TERA and WASSERBURG, 1972) concordia diagram (Fig. 5) all but two zircon samples from the gabbros show a linear array of data ellipses between apparent $^{206}Pb/^{238}U$ ages of 226 and 271 Ma. The two gabbros form distinct groups of data points, with the samples from Fed29 having higher apparent $^{238}U/^{206}Pb$ ages than those from BF202. Due to large errors most of the data ellipses overlap the concordia curve and appear concordant, but the individual data points in each of the two zircon populations do not form overlapping clusters. Therefore these are considered discordant. Abrasion did not yield data points plotting closer to a potential concordia intersection than unabraded zircons of the same rock. Two abraded samples even strongly deviate from the linear trend defined by all other gabbroic zircons. The former are characterised by the lowest contents of U and radiogenic Pb (BF202-15 and -16) and hence their U/Pb data might suggest an inadequate common lead correction. However, the measured raw $^{207}Pb/^{206}Pb$ ratio of sample BF202-16 cannot be corrected so to align with the discordia defined by the other samples if common lead with a realistic composition is used. This sample and BF202-15, characterised by an apparent $^{206}Pb/^{238}U$ age of approx. 340 Ma, suggest the presence of inherited lead.

The six data points of the gabbro sample Fed29 show only minor spread. Best fit regression (YORK, 1969) applied by program "Isoplot" of LUDWIG (1991) yields a lower concordia intersec-

Tab. 2 Zircon: Sample characteristics, U and Pb concentrations.

Sample	characteristics	weight [microg]	± %	U [ppm]	cl (total) [pg]	Pb blank [pg]	cl (sample) [pg]	cl (sample) [ppm]	Pb* [ppm]
Fed 29									
2	pale br., stubby	23.51	2.21	109	10.86	10	0.86	0.03658	5.37
4	colourless, equant	18.71	2.78	54	20.52	12	8.52	0.45537	2.63
6	br.-pk., stubby	29.46	1.77	112	33.95	12	21.95	0.74508	5.43
8	br.-pk., short.-prism., euh., abr.	19.45	2.67	149	26.15	12	14.15	0.72751	7.34
10c	pale br., abr., 3 cry.	14.44	17.2	119	26.5	12	14.5	1.00416	5.79
11a	clear, colourless, abr., 12 cry.	63.19	5.81	138	14.85	12	2.85	0.0451	6.74
BF 202									
5	red, equant-platy	19.18	5.21	46	56.35	12	44.35	2.3123	2.17
6	br.-grey	71.22	0.63	74	21.8	12	9.8	0.1376	3.36
7	grey-br., hemihedral	75.75	2.77	59	53.12	12	41.12	0.54284	2.79
9	red, fragment	48.57	1.3	77	15.58	12	3.58	0.07371	3.71
10	pale red, rugged surface	34.3	0.93	37	17.35	12	5.35	0.15598	1.92
15	white, partly embayed, abr.	27.96	2.8	6.6	20.97	12	8.97	0.32082	0.62
16	white, embayed, abr.	23.41	1.92	13.3	8.82	8	0.82	0.03503	0.51
17	yel., platy, cracked, abr.	29.97	2.3	60	13.46	12	1.46	0.04872	2.2
18	yel., abr.	36.8	2.5	33	20.9	12	8.9	0.24185	1.26
19	br, embayed, abr.	28.31	5.22	149	14.07	12	2.07	0.07312	5.08
27	pk.-br., embayed, cracks	32.3	17.65	78	12.27	12	0.27	0.00836	3.85
LP94									
1	clear, red, necked, round. edges	27.74	2.16	1240	29.2	12	17.2	0.62004	50.3
3	yel.-br., necked, round. edges	14.89	7.59	1256	24.4	12	12.4	0.83277	51.4
4	reddish, abr.	13.02	3.3	1747	49	12	37	2.84178	67.1
5	reddish, abr.	7.88	6.85	1446	19.6	12	7.6	0.96447	56.5
7	white, turbid, crack, abr.	24.57	1.59	806	59.6	12	47.6	1.93732	33
8	colourless, clear, crack,abr.	29.71	1.46	830	67.3	12	55.3	1.86133	34.8
10	light brown, turbid	34.3	1.87	4026	633.3	15	618.3	18.0262	108
13	clear, yel., embayed	10.2	5.78	1344	77.5	12	65.5	6.42157	53
17	light pink, embayed	24.2	2.31	656	47.8	12	35.8	1.47934	27.4
18	light pk.-ppl.	18.2	6.04	831	92.8	12	80.8	4.43956	35.4
19	light yel., turbid, broken	14.7	7.48	615	25.7	12	13.7	0.93197	24.2

Abbreviations:
abr. = abraded; br. = brown; cl = common lead; Pb* = radiogenic lead; cry. = crystals; euh. = euhedral; gr. = grey; pk. = pink; ppl. = purple; yel = yellow.

tion age of 257 ± 17 Ma and an upper intersection at 517 ± 590 Ma and an MSWD value of 1.14. All data points fall close to the lower concordia intersection, which is interpreted as the intrusion age of this gabbro. Note, however, that in this scenario two data points would be concordant, whereas the four other slightly discordant zircon data points suggest the presence of inherited lead. This is considered as very unlikely (see section 7.3). Furthermore, the direction of the regression is strongly influenced by sample Fed29-4 characterised by a raw $^{206}Pb/^{204}Pb$ ratio of only 151 which, therefore, is very sensitive to common lead correction and may reflect problems therein. Exclusion of this sample yields a best fit regression which locally is nearly parallel to the concordia curve having intersections at 241 ± 180 Ma and 334 ± 550 Ma.

Regression of the data points of sample BF202 excluding BF202-15 and BF202-16 results in an lower intersection age of 185 ± 72 and a upper intersection age at 319 ± 100 Ma (MSWD = 1.4) on the Tera-Wasserburg concordia diagram. Alternatively for data corrected with 100 Ma model common lead (STACEY and KRAMERS, 1975), the corresponding intersection ages would be 188 ± 99 Ma and 328 ± 160 Ma, respectively (MSWD = 1.6). If only the samples with measured $^{206}Pb/^{204}Pb$ ratios >300 are used for regression the following intersections result: 188 ± 71 Ma and 325 ± 120 Ma (MSWD = 1.02).

Zircons from the anatectic leucogranite strongly differ from the gabbroic zircons by their elevated U and radiogenic Pb contents (~1000 ppm) and significantly smaller errors of the data

Tab. 3 Zircons: U/Pb isotopic results.

Sample	238U [picomoles] (a,b)	206Pb* [picomoles] (a,c)	206Pb/204Pb (b)	207Pb*/206Pb* (a,c)	208Pb*/206Pb* (a,c)	238U/206Pb* (a,c)	207Pb*/235U (a,c)	ρ (d)
Fed 29								
2	10.704 (46)	0.4461 (16)	641	0.05191 (57)	0.3182 (17)	23.99 (12)	0.2983 (38)	–0.159
4	4.202 (19)	0.1801 (8)	151	0.0531 (14)	0.2688 (47)	23.33 (13)	0.3139 (90)	–0.36
6	13.780 (59)	0.5645 (19)	270	0.05148 (47)	0.3214 (16)	24.41 (11)	0.2908 (32)	–0.164
8	12.068 (52)	0.4937 (18)	304	0.05149 (62)	0.3491 (19)	24.44 (12)	0.2904 (40)	–0.165
10c	7.147 (31)	0.2984 (11)	189	0.05199 (92)	0.3062 (30)	23.95 (12)	0.2992 (59)	–0.248
11a	36.43 (16)	1.5265 (49)	1575	0.05165 (17)	0.3000 (6)	23.87 (11)	0.2984 (17)	–0.057
BF202 (e)								
5	3.683 (16)	0.1456 (8)	57.9	0.0535 (26)	0.3509 (71)	25.30 (16)	0.291 (15)	–0.471
6	22.048 (94)	0.8200 (27)	595	0.05119 (32)	0.3608 (11)	26.89 (12)	0.2625 (21)	–0.113
7	18.607 (80)	0.7321 (25)	230	0.05154 (44)	0.3480 (14)	25.42 (12)	0.2796 (29)	–0.132
9	15.529 (66)	0.6120 (21)	621	0.05173 (42)	0.3729 (14)	25.37 (12)	0.2811 (28)	–0.136
10	5.301 (23)	0.2128 (9)	206	0.0514 (12)	0.4476 (38)	24.90 (13)	0.2844 (72)	–0.316
15	0.775 (7)	0.0426 (20)	49.8	0.072 (36)	0.911 (57)	18.21 (87)	0.54 (30)	–0.957
16	1.302 (6)	0.0447 (5)	95.1	0.0698 (78)	0.224 (21)	29.12 (37)	0.330 (40)	–0.779
17	6.983 (30)	0.2485 (10)	301	0.0518 (11)	0.1429 (39)	28.10 (14)	0.2544 (57)	–0.296
18	5.018 (22)	0.1927 (10)	160	0.0544 (27)	0.1189 (68)	26.05 (16)	0.288 (15)	–0.432
19	17.592 (75)	0.6277 (21)	701	0.05104 (42)	0.0604 (15)	28.03 (13)	0.2511 (25)	–0.137
27	10.545 (46)	0.4248 (15)	550	0.05171 (59)	0.3662 (20)	24.83 (12)	0.2872 (38)	–0.181
LP94-T37								
1	143.51 (62)	6.080 (20)	3207	0.05174 (6)	0.0619 (2)	23.60 (11)	0.3023 (14)	–0.02
3	77.98 (33)	3.294 (11)	2086	0.05182 (10)	0.0757 (4)	23.67 (11)	0.3018 (15)	–0.065
4	94.85 (41)	3.848 (13)	1222	0.05166 (10)	0.0495 (4)	24.65 (12)	0.2889 (15)	–0.073
5	47.54 (20)	1.9511 (64)	1547	0.05160 (14)	0.0558 (6)	24.37 (11)	0.2920 (16)	–0.04
7	82.57 (59)	3.416 (22)	896	0.05156 (24)	0.1009 (7)	24.17 (11)	0.2941 (20)	–0.092
8	102.81 (44)	4.395 (14)	1019	0.05182 (8)	0.0874 (3)	23.39 (11)	0.3054 (15)	–0.002
10c (f)	575.9 (40)	16.21 (10)	628	0.05065 (7)	0.0573 (2)	35.54 (16)	0.1965 (10)	–0.189
13	57.16 (41)	2.335 (15)	480	0.05397 (14)	0.0690 (6)	24.48 (11)	0.3040 (17)	–0.091
17	66.22 (53)	2.838 (21)	929	0.05166 (14)	0.0824 (5)	23.33 (11)	0.3053 (17)	–0.081
18	63.07 (21)	2.671 (10)	460	0.05173 (27)	0.1185 (7)	23.61 (10)	0.3021 (21)	–0.083
19	37.71 (19)	1.4875 (52)	907	0.05174 (24)	0.1099 (9)	25.36 (14)	0.2814 (20)	–0.051

Radiogenic lead is marked with an asterisk (*).
(a) Errors (2σ) are shown in brackets and refer to the last digits given.
(b) Corrected for mass fractionation and tracer contributions
(c) Corrected for mass fractionation, tracer contributions as well as sample and blank common lead.
(d) Correlation coefficient ρ for $^{238}U/^{206}Pb$- and $^{207}Pb/^{206}Pb$- errors.
(e) Pb composition of Fed29 plagiclase has been used for sample common Pb correction.
(f) Data combined for sample and leach solution.

points, otherwise they define a similar linear trend as the combined zircons from the gabbros. One of 11 grains strongly falls off the linear trend defined by the other 10 data points. This could be explained by inheritance which is expected in this anatexite derived from metapelitic source rocks containing old zircon components of an apparent age range between 450 and 3000 Ma (D. Rubatto, pers. comm.). A best fit regression through the ten points (MSWD = 1.3), excluding sample 13, yields a lower intersection age of 99.8 –6.5/+6.3 Ma and an upper intersection at 278.4 –2.5/+2.6 Ma.

7. Discussion

7.1. U/PB SYSTEMATICS OF ZIRCON

The discordance of zircons from the three rocks which have undergone the same post-magmatic history cannot be explained by a simple Pb-loss process alone for the following reasons. (1) The analysed zircons show no correlation between their degree of discordance and their U contents (e.g. SILVER and DEUTSCH, 1963), neither if zircon populations of the different rocks are compared to one another nor if zircons of one specific rock are compared. For example, most of the U-rich (600–1700 ppm) zircons from the leucogranite show the same degree of discordance as the U-poor zircons (30–80 ppm) from the Ti-Fe-gabbro BF202. This is best explained by variable Alpine metamorphic overprint involving fluids as documented by their different hydrous mineral assemblages. On the other hand, samples 17 and 19 from the same sample BF202 show nearly identical discordance, but they differ in their U contents by a factor of 2.5. This could be due to other effects superimposed on the Pb loss during Alpine metamorphism. For example the cracking/healing processes may have affected the U/Pb systems of individual zircons in a different way. (2) Abrasion, a technique applied to remove the often U-rich zircon rims which tend to lose radiogenic lead (KROGH, 1982), did not yield more concordant data than unabraded zircon grains. This observation suggests that the zircons dated are characterised by a zoning different from the often observed U enrichment in outer zones. CL imaging indeed revealed that the studied zircons bear a more complex internal structure and are composed of two major generations of zircon formation/recrystallisation (Fig. 4). A thorough investigation of the structure of these zircons, their chemical characteristics and the effects concerning their U/Pb system will be discussed in a separate paper.

7.2. GEOLOGICAL SIGNIFICANCE OF THE AGE RESULTS

Best fit regressions for the zircon data of both gabbros intersect the concordia curve with large error margins. Therefore, only imprecise age information can be derived from these data. Lower and upper regression intersection ages on the Tera-Wasserburg curve obtained for the two gabbros even appear to be markedly different (lower intersection: Fed29 = 257 Ma, BF202 = 185–188 Ma; upper intersection: Fed29 = 517, BF202 = 319–328 Ma) though their large errors bands overlap. However, field evidence (MÜNTENER and HERMANN, 1996) and geochemical relations (HERMANN et al., 2001) indicate that the two gabbros are part of the same igneous complex, and hence only a minor difference between their intrusion ages is expected. A best fit regression combining the gabbro zircons (excluding BF202-15 and -16, MSWD = 1.3) yields a lower intersection with the concordia curve at 143 ± 71 Ma and an upper intersection at 281 ± 19 Ma. Using only the samples with raw $^{206}Pb/^{204}Pb > 300$ the corresponding intersection ages is 142 ± 73 Ma and 279 ± 19 Ma (MSWD = 0.85). Applying 100 Ma model common lead (STACEY and KRAMERS, 1975) for the correction of the BF202 zircon results in slightly different lower intersection ages of 138 ± 93 Ma and 139 ± 73 Ma, respectively.

Note that all data points of Fed29 fall on the regression line for combined gabbro data and do not suggest presence of inheritance, as has been discussed in section 6. Such data treatment also takes into account the textural observations in the zircons. All grains display clearly post-magmatic recrystallisation as documented by CL images as well as by healed cracks, whereas there is little evidence for widespread inheritance (see below). It is likely that all grains underwent minor lead loss during the Alpine event. Hence, a discordia with a lower intersection representing the Alpine metamorphism and an upper intersection representing the magmatic age is in good agreement with the zircon structure and the geological context.

The regression line obtained for zircons from the combined gabbro samples overlaps within error limits with the more precisely defined discordia of the anatectic leucogranite for which the upper intersection of 278 –2.5/+2.6 Ma represents the age of the anatexis and the lower intersection points to an Alpine event. For the gabbros the upper intersection age is interpreted to give the age of intrusion whereas the less well defined lower intersection may either suggest an Alpine or earlier exhumation-related overprint.

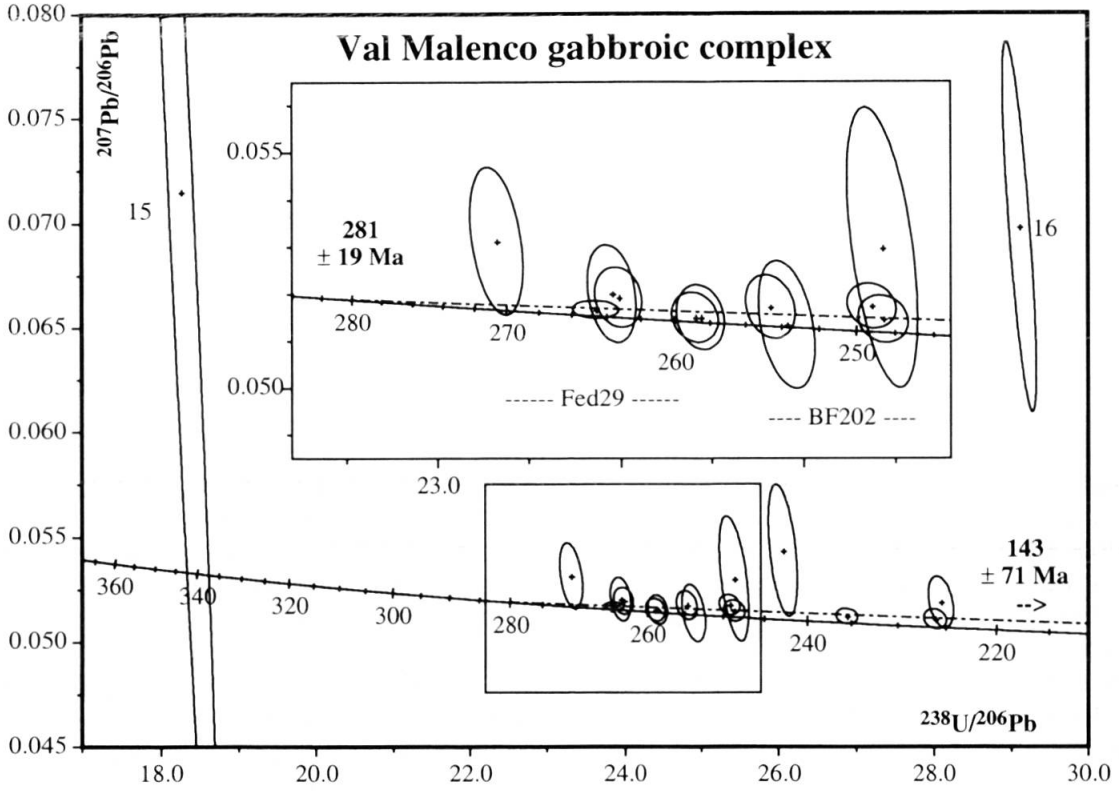

Fig. 5 Tera-Wasserburg concordia diagram for gabbroic zircon data. The inset shows an enlargement of the area outlined by the rectangle. Error ellipses correspond to the 95% confidence limits. Only the best fit regression for the combined gabbro data is shown (see text).

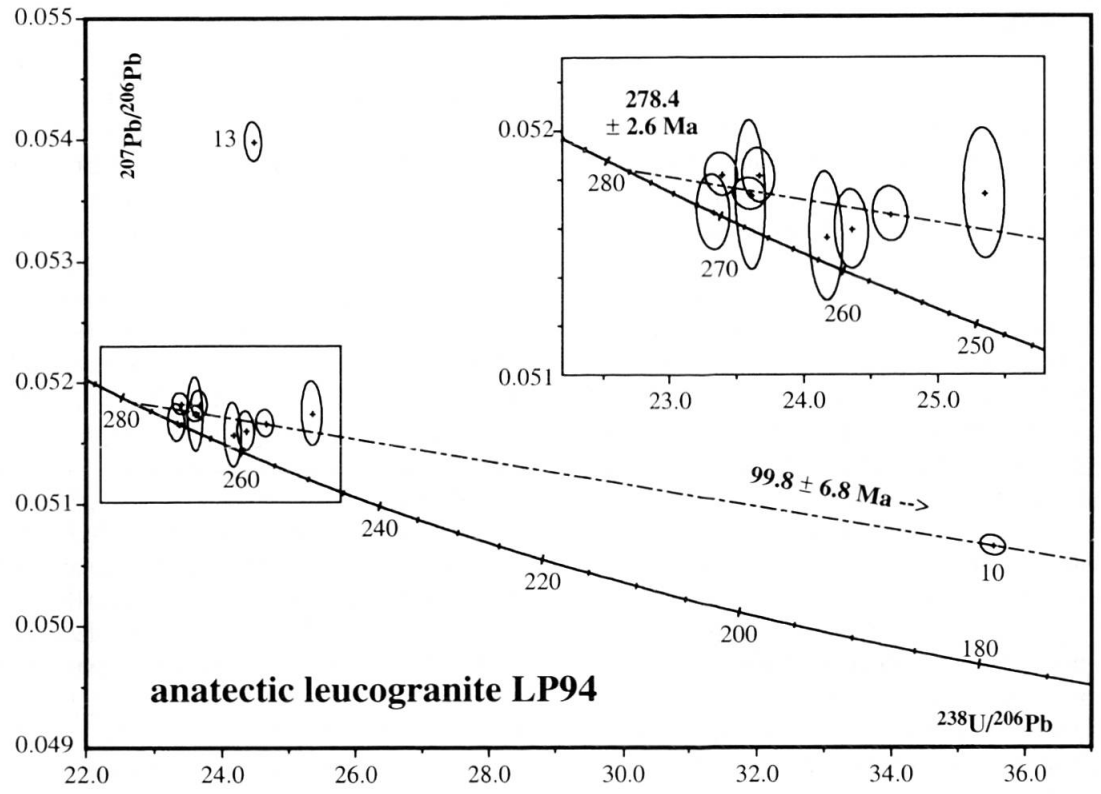

Fig. 6 Tera-Wasserburg concordia diagram showing zircon data of the anatectic leucogranite. Data points strongly deviating from the majority of the zircons are labelled with their sample number. No. 10 is characterised by a U content of about 4000 ppm and No. 13 most likely contained an unrecognised inherited core. The inset shows an enlargement of the area outlined by the rectangle.

The overlapping upper concordia intersection ages of 281 ± 19 Ma obtained for the gabbro intrusion and of 278 –2.5/+2.6 Ma for the anatectic leucogranite are in agreement with field relations that strongly suggest that partial anatexis of metapelites was caused by the intrusion of the gabbros, and these two events therefore were nearly coeval. The more precise age of 278 –2.5/+2.6 Ma obtained from the anatectic leucogranite is considered a good approximation of the intrusion age of the gabbros. We also note that the thermal metamorphic peak registered by the lower crustal rocks of the Malenco unit reflects a Permian event rather than the Variscan orogeny.

The age of 278 –2.5/+2.6 Ma is very similar to the zircon U/Pb ages of 285 Ma determined for a diorite (PIN, 1986) and 293 ± 6 Ma for a metagabbro (VAVRA et al., 1999) of the Ivrea zone and the 270 Ma obtained for the Sondalo gabbroic complex (BACHMANN and GRAUERT, 1981). The age determined for the Malenco gabbros further supports the hypothesis of a post Variscan, Early Permian phase of extension (e.g. DAL PIAZ, 1993) which is indicated by several deep crustal gabbroic intrusions.

The lower concordia intersection age of 99.8 –6.5/+ 6.3 Ma is slightly older than the range of 83–91 Ma determined on zoned amphiboles of Malenco rocks (VILLA et al., 2000) which was interpreted to reflect an early pressure dominated phase of Alpine metamorphism. Early thrusting at the Penninic-Austroalpine boundary has been estimated at about 90–110 Ma (HANDY et al., 1996) on the basis of geological arguments. On a microscopic scale, the Alpine metamorphic event is reflected by the high CL recrystallisation domains and rims of the zircons (Fig. 4).

The zircons of the three rocks have also registered at least one strong deformation, which caused cracking and breaking of many crystals particularly in the Ti-Fe-gabbro BF202. Most of the cracks were healed in the presence of fluid but they are still recognisable by the internal surfaces filled with fluid inclusions. As the effective events could be considered either the post intrusive deformation leading to the flasergabbro (GAUTSCHI, 1980; HERMANN and MÜNTENER, 1996) or processes during the Alpine collision. Healing of the cracks required the presence of fluids and most likely was accompanied by lead loss from zircon. This process took place either during hydrous retrograde metamorphism in the course of the exhumation of the Malenco crust-to-mantle transition or during Alpine metamorphism. The U/Pb results of gabbro BF202 do not allow a conclusive statement on the timing of this event.

7.3. ZIRCON INHERITANCE

Some zircons appear to be "exotic". The data points of several grains (e.g. BF202-16, LP94-13) clearly plot off the linear trend defined by the majority of the zircons. One zircon grain (BF202-15) is even characterised by an apparent $^{206}Pb/^{238}U$ age of about 340 Ma.

In the anatectic leucogranite LP94 cores in the zircons were detected by CL imaging (Fig. 4b) which could be explained by residual grains that survived melting. A melt with the chemical composition of this rock (HERMANN, 1997) is saturated with zircon at a temperature below about 870 °C using the zircon saturation model of WATSON and HARRISON (1983). Thermobarometric estimates of the conditions during the granulite grade reequilibration of the lower crustal Malenco rocks following the gabbroic intrusion yield a temperature range between 750 and 850 °C (MÜNTENER et al., 2000). Thus, the leucocratic anatectic melt most likely was saturated with zircon and a part of the preexisting zircons may have survived melting.

Cores were not detected in the gabbroic zircons by optical means and by CL imaging. Presence of inherited crustal components in zircon of the gabbroic complex seems rather unlikely given the intrusion level at the immediate crust-to-mantle boundary. The generally low zircon contents in these gabbros indicates that their magmas most likely did not reach zircon saturation during crystallisation. Xenocrystic zircons probably would not have survived. The Ti-Fe-gabbro BF202 differs strongly from the other gabbros. Abundant zircons and a high Zr content in this rock indicate that its magma attained zircon saturation and thus xenocrystic zircon could have survived. Based on Pb isotope data and field relations crustal contamination in the other Ti-Fe-gabbro PF202 is obvious, whereas it is rather unlikely for Ti-Fe-gabbro BF202, which is located within the gabbroic body.

A mantle origin of the "exotic" grains (BF202-15, BF202-16) is consistent with their low U contents (e.g. DAVIS, 1978). Furthermore some evidence exists that zircon in the mantle may retain some radiogenic Pb (KINNY et al., 1989; SCHÄRER et al., 1997). Mantle-derived zircon, if present, could not be distinguished optically from the gabbroic zircon. Original differences between two groups of zircon, which both never showed ideal crystal forms, might have been further obscured by later cracking and healing. However, it is unlikely that zircon either had survived the extreme conditions of partial melting at the magma source in the mantle or that zircon was residual from

mantle xenoliths digested by the zircon undersaturated tholeiitic magma.

7.4. LEAD ISOTOPIC SIGNATURE OF PLAGIOCLASE

Plagioclase separated from the major gabbro types display elevated μ and ω values compared to MORB and suggest the presence of crustal Pb components. Admixture of crustal material to gabbroic magma prior to its differentiation would be consistent with the fairly homogeneous Pb isotope compositions of most of the different gabbro types. This could best be explained by contamination at the magma source in the mantle. Conversely, a combined process of crustal assimilation and magmatic differentiation at the crust-to-mantle boundary would produce differentiates with Pb isotopic compositions systematically changing towards the crustal assimilate which, however, is not observed in the studied samples. It cannot be ruled out a priori that later interactions with fluids during metamorphism affected the Pb isotopic compositions of plagioclase. However, interactions with fluids were restricted to their pathways, where the rocks show alteration, but they were not pervasive as indicated by the primary mineralogy which still is preserved. Since fluid alteration had affected the different samples to variable degrees, some mixing array of the data between two end members would be expected rather than the observed data cluster.

The Pb isotopic characteristics of the studied gabbros are very similar to those of silicates and sulphides from mafic rocks of the Ivrea zone (CUMMING et al., 1987). These authors concluded that the observed relatively high μ and ω values reflect the mantle source of the magmas, which they considered to be contaminated by subducted material.

Interestingly, the Permian tholeiitic Mg- and Fe-gabbros are characterised by crustal μ and ω values that differ clearly from Jurassic MOR type basalts represented by the amphibolites of the Forno unit (PERETTI and KÖPPEL, 1986). Despite the close spatial association of these two groups of tholeiitic rocks their Pb isotopic signatures suggest different mantle sources.

8. Summary and conclusions

U–Pb dating on single zircons of different members from the tholeiitic Braccia gabbro suite revealed to be a challenging task. Near complete absence or very low yields of zircon in the major rock types (Mg- and Fe-gabbros) required to direct the search for zircons to samples in which they had been detected microscopically and/or were directly related to the gabbroic intrusion. Thus zircons were separated from a highly differentiated Ti-Fe-gabbro despite its Alpine metamorphic mineralogy. Further samples of this rock type from the studied gabbro complex were also characterised by the highest Zr contents (HERMANN, 1997; HERMANN et al., 2001) and therefore this rock type appeared as the most promising candidate in the search for zircons. Such highly differentiated rocks are, however, relatively rare and not easily distinguished from Fe-gabbros in the field. Further zircons were separated from a leucogranite generated by partial wall rock melting during the intrusion of the gabbros. This approach of indirectly dating the gabbro intrusion was possible because local partial melting took place within the contact aureole.

CL imaging (Figs 4a, b) revealed that all the zircons are built of two generations of zircon formation/recrystallisation, which are represented by (a) oscillatory zoned magmatic zircon centres and (b) rims and replacement domains characterised by bright CL intensity. The latter are interpreted to result from recrystallisation during Alpine metamorphism.

The U/Pb results of some gabbroic zircons suggest the presence of inheritance in a Ti-Fe-gabbro of this tholeiitic suite at the crust-mantle boundary. Due to the high Zr contents its magma may have been saturated with zircon and thus xenocrystic zircon may have survived. Cores or xenocrysts, however, could not be detected by optical means or CL imaging, and field relations and geochemistry do not support the hypothesis of crustal assimilation.

The combined zircon data from the two gabbros and zircons from the leucogranite yield overlapping discordia lines with upper intersection ages of 281 ± 19 Ma and 278 –2.5/+2.6 Ma, respectively. The age of 278 Ma therefore is considered as the age of the gabbroic emplacement which caused granulite-grade metamorphism in the lower crustal country rocks intruded by the gabbros. The Early Permian age of the Malenco gabbroic complex suggests that it reflects the same post-Variscan extension-related cycle of deep crustal mafic magmatism as other major gabbros in the Alps as those of the Ivrea zone and near Sondalo in the Southern Alps. The Malenco gabbros and associated rocks were exhumed during Jurassic rifting and emplaced along a continent-ocean transition of the Tethyan ocean.

The close association of ultramafic rocks, gabbros and basalts with a Jurassic sedimentary cover

in Val Malenco has long been regarded as an example for a classical ophiolite sequence. However, the mafic intrusives are separated in time (Permian vs. Jurassic) and crystallised at different pressures (1 GPa vs. <0.1 GPa), and had different magma sources as indicated by their different Pb isotopic composition. The mafic rocks from Val Malenco thus clearly show that exhumation of lithospheric mantle and lower crust was a major process during the formation of a passive continental margin.

Acknowledgements

We thank V. Trommsdorff for stimulating the interesting and facet-rich work in the Monte Braccia area (Val Malenco). W. H. acknowledges financial support from Swiss NF grant No. 21-36113.92. Th. Ulrich is thanked for providing the zircon-rich leucogranite sample. Two anonymous reviewers provided valuable and critical comments leading to major improvements of the manuscript.

References

BACHMANN, G. and GRAUERT, B. (1981): Radiometrische Altersbestimmung des Gabbros von Sondalo, Oberes Veltlin, Italienische Alpen. Fortschr. Mineral. 59, Beihefte, 11–12.

BEARTH, P. (1967): Die Ophiolithe der Zone Zermatt–Saas Fee. Beitr. geol. Karte Schweiz N.F. 132.

BOSSART, P.J., MEIER, M., OBERLI, F. and STEIGER, R.H. (1986): Morphology versus U–Pb systematics in zircon: a high-resolution isotopic study of a zircon population from a Variscan dike in the Central Alps. Earth Planet. Sci. Lett. 78, 339–354.

BURKHARD, D. and O'NEILL, J. (1988): Contrasting serpentinization processes in the eastern Central Alps. Contrib. Mineral. Petrol. 99, 498–506.

CUMMING, G.L., KÖPPEL, V. and FERRARIO, A. (1987): A lead isotope study of the northeastern Ivrea zone and adjoining Ceneri zone (N-Italy): evidence for a contaminated subcontinental mantle. Contrib. Mineral. Petrol. 97, 19–30.

DAL PIAZ, G. V. (1993): Evolution of Austro-Alpine and upper Penninic basement in the Northwestern Alps from Variscan convergence to Post-Variscan extension. In: VON RAUMER J.F. and NEUBAUER F. (eds): Pre-Mesozoic Geology in the Alps, Springer Verlag, 327–344.

DAVIS, G.L. (1978): Zircons from the mantle. Short papers of the IV international conference, geochronology, cosmochronology, isotope geology. USGS Open file report 78-701, 86–88.

DESMURS, L., MANATSCHAL, G. and BERNOULLI, D. (2001): The Steinmann Trinity revisited: mantle exhumation and magmatism along an ocean-continent transition: the Platta nappe, eastern Switzerland. In: WILSON, R.C.L., WITHMARSH, R.B., TAYLOR, B. and FROITZHEIM, N. (eds): Non-volcanic rifting of continental margins: a comparison of evidence from land and sea. Geol. Soc. London Spec. Publ. 187, in press.

DEUTSCH, A. (1983): Datierungen an Alkaliamphibolen und Stilpnomelan aus der südlichen Platta-Decke (Graubünden). Eclogae geol. Helv. 76, 295–308.

DIETRICH, V. (1969): Die Ophiolithe des Oberhalbsteins (Graubünden) und das Ophiolithmaterial der ostschweizerischen Molasse, ein petrographischer Vergleich. Europäische Hochschulschriften, Reihe 17: Erdwissenschaften 1, 179 pp.

FERRARIO, A. and MONTRASIO, A. (1976): Manganese ore deposits of Monte del Forno. Schweiz. Mineral. Petrogr. Mitt. 56, 377–385.

GAUTSCHI, A. (1979): Geologie und Petrographie des Fedozer Gabbros (Östliche Zentralalpen: Prov. Sondrio, N-Italien/ Kt. Graubünden, Schweiz). Schweiz. Mineral. Petrogr. Mitt. 59, 423–427.

GAUTSCHI, A. (1980): Metamorphose und Geochemie der basischen Gesteine des Bergeller Ostrands. Ph.D. thesis ETH Zurich, 170 pp.

GUNTLI, P. and LINIGER, M. (1989): Metamorphose der Margna-Decke im Bereich Piz da la Margna und Piz Fedoz. Schweiz. Mineral. Petrogr. Mitt. 69, 289–301.

GYR, T. (1967): Geologische und petrographische Untersuchungen am Ostrande des Bergeller Massivs. Ph.D. thesis ETH Zurich, 125 pp.

HANDY, M.R., HERWEGH, M., KAMBER, B.S., TIETZ, R. and VILLA, I.M. (1996): Geochronologic, petrologic, and kinematic constraints on the evolution of the Err-Platta boundary, part of a fossil continent-ocean suture in the Alps (eastern Switzerland). Schweiz. Mineral. Petrogr. Mitt. 76, 453–474.

HERMANN, J. and MÜNTENER, O. (1996): Extension-related structures in the Malenco-Margna-system: implications for paleogeography and consequences for rifting and Alpine tectonics. Schweiz. Mineral. Petrogr. Mitt. 76, 501–519.

HERMANN, J., MÜNTENER, O., TROMMSDORFF, V., HANSMANN, W. and PICCARDO, G.B. (1997): Fossil crust-to-mantle transition, Val Malenco (Italian Alps). J. Geophys. Res. 102, 20123–20132.

HERMANN, J. (1997): The Braccia gabbro (Malenco, Alps): Permian intrusion at the crust to mantle interface and Jurassic exhumation during rifting. Ph.D. thesis ETH Zurich, 194 + 39A pp.

HERMANN, J., MÜNTENER, O. and GÜNTHER, D. (2001): Differentiation of mafic magma in a continental crust-to-mantle transition zone. J. Petrol. 42, 189–206.

HUNZIKER, J.C., DESMONS, J. and HURFORD, A.J. (1992): Thirty-two years of geochronological work in the Central and Western Alps: a review on seven maps. Mém. Géologie (Lausanne) 13, 59 pp.

JÄGER, E. and HUNZIKER, J. (1969): Geochronology of Phanerozoic Orogenic Belts. Guide Book, Field Trip Switzerland.

KINNY, P.D., COMPSTON, W., BRISTOW, J.W. and WILLIAMS, I.S. (1989): Archean mantle xenocrysts in a Permian kimberlite: Two generations of kimberlitic zircon in Jwaneng DK2, southern Botswana. Geol. Soc. Austr. Spec. Publ. 14, 833–842.

KÖPPEL, V., HANSMANN, W. and MAGGETTI, M. (1997): Pb isotope and trace element signatures of polymetamorphic rocks from the Silvretta nappe, a comparison. Schweiz. Mineral. Petrogr. Mitt. 77, 325–335.

KROGH, T.E. (1973): A low contamination method for the hydrothermal decomposition of zircon and extraction of U and Pb for isotopic age determinations. Geochim. Cosmochim. Acta 37, 485–494.

KROGH, T.E. (1982): Improved accuracy of U–Pb zircon ages by the creation of a more concordant system using air abrasion technique. Geochim. Cosmochim. Acta 46, 637–649.

LEMOINE, M., TRICART, P. and BOILLOT, G. (1987): Ultramafic and gabbroic ocean floor of the Ligurian Tethys (Alps, Corsica, Apennines): In search of a genetic model. Geology 15, 622–625.

LUDWIG, K.R. (1991): Isoplot – a plotting and regression program for radiogenic isotope data. USGS Open file report 91-445.

MONJOIE, P., BUSSY, F., SCHALTEGGER, U., LAPIERRE, H. and PFEIFER, H.R. (2001): Permian mafic rocks in the Alps: A post-orogenic mantle melting event illustrated by the Mont Collon-Matterhorn intrusion (Austroalpine Dent-Blanche nappe). Strasbourg, J. Conf. Abs. 6, p. 475.

MONTRASIO, A. (1973): Strutture a pillow nelle anfiboliti del M. del Forno (Pennidico medio – Alpi Retiche). Atti Acc. Naz. Lin. Rend. Sci. fis. mat. nat. 54, 114–123.

MÜNTENER, O. and HERMANN, J. (1996): The Val Malenco lower crust-upper mantle complex and its field relations (Italian Alps). Schweiz. Mineral. Petrogr. Mitt. 76, 475–500.

MÜNTENER, O., HERMANN, J. and TROMMSDORFF, V. (2000): Cooling history and exhumation of lower crustal granulite and upper mantle (Malenco, Eastern Central Alps). J. Petrol. 41, 175–200.

OBERLI, F., SOMMERAUER, J. and STEIGER, R.H. (1981): U–(Th)–Pb systematics of single crystals and concentrates of accessory minerals from the Cacciola granite, central Gotthard massif, Switzerland. Schweiz. Mineral. Petrogr. Mitt. 61, 323–348.

PERETTI, A. (1985): Der Monte-del-Forno-Komplex am Bergell-Ostrand: Seine Lithostratigraphie, alpine Tektonik und Metamorphose. Eclogae geol. Helv. 78, 23–48.

PERETTI, A. and KÖPPEL, V. (1986): Geochemical and lead isotope evidence for a mid-ocean ridge type mineralization within a polymetamorphic ophiolite complex (Monte del Forno, North Italy/Switzerland). Earth Planet. Sci. lett. 80, 252–264.

PIN, C. (1986): Datation U–Pb sur zircons à 285 M.a. du complexe gabbro-dioritique du Val Sesia-Val Mastallone et âge tardi-hercynien du métamorphisme granulitique de la zone Ivrea-Verbano (Italie). C.R. Acad. Sc. Paris 303, 827–829.

POLDERVAART, A. (1956): Zircons in rocks. 2. Igneous rocks. Am. J. Sci. 254, 521–554.

POZZORINI, D. and FRUEH-GREEN, G. (1996): Stable isotope systematics of the Ventina ophicarbonate zone, Bergell contact aureole. Schweiz. Mineral. Petrogr. Mitt. 76, 549–564.

PUSCHNIG, A.R. (2000): The oceanic Forno unit (Rhetic Alps): field relations, geochemistry and paleogeographic setting. Eclogae geol. Helv. 93, 103–124.

RODDICK, J. C. (1987): Generalised numerical error analytics with application to geochronology and thermodynamics. Geochim. Cosmochim. Acta 51, 2129–2135.

RUBATTO, D., GEBAUER, D. and FANNING, M. (1998). Jurassic formation and Eocene subduction of the Zermatt–Saas Fee ophiolites: implications for the geodynamic evolution of the Central and Western Alps. Contrib. Mineral. Petrol. 132, 269–287.

RUBATTO, D., GEBAUER, D. and COMPAGNONI, R. (1999): Dating of eclogite-facies zircons: the age of Alpine metamorphism in the Sesia-Lanzo Zone (Western Alps). Earth Planet. Sci. Lett. 167, 141–158.

SCHÄRER, U., CORFU, F. and DEMAIFFE, D. (1997): U–Pb and Lu–Hf isotopes in baddeleyite and zircon megacrysts from the Mbuji-Mayi kimberlite: constraints on the subcontinental mantle. Chem. Geol. 143, 1–16.

SILVER, L.T. and DEUTSCH, S. (1963): Uranium-lead isotopic variations in zircons: a case study. J. Geol. 71, 721–758.

SPILLMANN, P. (1989): Struktur und Metamorphose der Margna-Decke im obersten Valmalenco. Schweiz. Mineral. Petrogr. Mitt. 69, 147–150.

SPILLMANN, P. (1993): Die Geologie des penninisch-ostalpinen Grenzbereichs im südlichen Berninagebirge. Ph.D. thesis ETH Zurich, 262 pp.

SPILLMANN, P. and BÜCHI, H.J. (1993): The pre-Alpine basement of the lower Austro-Alpine nappes in the Bernina Massif (Grisons, Switzerland; Valtellina, Italy). In: VON RAUMER J.F. and NEUBAUER F. (eds): Pre-Mesozoic Geology in the Alps, Springer Verlag, 457–467.

STACEY, J.S. and KRAMERS, J.D. (1975): Approximation of terrestrial lead isotope evolution by a two-stage model. Earth Planet. Sci. Lett. 16, 207–221.

STAUB, R. (1922): Ueber die Verteilung der Serpentine in den alpinen Ophiolithen. Schweiz. Mineral. Petrogr. Mitt. 2, 78–149.

STAUB, R. (1946): Geologische Karte der Berninagruppe 1:50'000. Spez. Karte Nr. 118, Schweiz. Geol. Kommission.

TERA, F. and WASSERBURG, G.J. (1972): U–Th–Pb systematics in Lunar highland samples from the Luna 20 and Apollo 16 missions. Earth Planet. Sci. Lett. 17, 36–51.

TRIBUZIO, R., THIRLWALL, M.F. and MESSIGA, B. (1999): Petrology, mineral and isotope geochemistry of the Sondalo gabbroic complex (Central Alps, Northern Italy): implications for the origin of post-Variscan magmatism. Contrib. Mineral. Petrol. 136, 48–62.

TROMMSDORFF, V. and EVANS, B.W. (1977): Antigorite ophicarbonates: Contact metamorphism in Val Malenco. Contrib. Mineral. Petrol. 62, 301–312.

TROMMSDORFF, V., PICCARDO, G.B. and MONTRASIO, A. (1993): From magmatism through metamorphism to sea floor emplacement of subcontinental Adria lithosphere during pre-Alpine rifting (Malenco, Italy). Schweiz. Mineral. Petrogr. Mitt. 73, 191–203.

ULRICH, T. and BORSIEN, G.-R. (1996): Fedozer Metagabbro und Forno-Metabasalt (Val Malenco, Norditalien): Vergleichende petrographische und geochemische Untersuchungen. Schweiz. Mineral. Petrogr. Mitt. 76, 521–535.

VAVRA, G., SCHMID, R. and GEBAUER, D. (1999): Internal morphology, habit and U–Th–Pb microanalysis of amphibolite-to-granulite facies zircon: geochronology of the Ivrea zone (Southern Alps). Contrib. Mineral. Petrol. 134, 380–404.

VILLA, I.M., HERMANN, J., MÜNTENER, O. and TROMMSDORFF, V. (2000): ^{39}Ar–^{40}Ar dating of multiply zoned amphibole generations (Malenco, Italian Alps). Contrib. Mineral. Petrol. 140, 363–381.

VOSHAGE, H., HOFMANN, A.W., MAZZUCCHELLI, Q.M., RIVALENTI, G., SINIGOI, S., RACZEK, I. and DEMARCHI, G. (1990): Isotopic evidence from the Ivrea zone for hybrid lower crust formed by magmatic underplating. Nature 347, 731–736.

WAGNER, G.A., REIMER, D.S. and JÄGER, E. (1977): Cooling ages derived by apatite fission-track, mica Rb–Sr and K–Ar dating: the uplift and cooling history of the Central Alps. Mem. Ist. Geol. Min. Univ. Padova 30, 1–30.

WATSON, E.B. and HARRISON, T.M. (1983): Zircon saturation revisited: temperature and composition effects in a variety of crustal magma types. Earth Planet. Sci. Lett. 64, 295–304.

YORK, D. (1969): Least squares fitting of a straight line with correlated errors. Earth Planet. Sci. Lett. 5, 320–324.

Manuscript received November 31, 2000; revision accepted July 7, 2001.
Editorial handling: M. Cosca